

## Forces between Conducting Surfaces due to Spatial Variations of Surface Potential

C. C. Speake and C. Trenkel

*Gravitation Group, School of Physics and Astronomy, University of Birmingham, Birmingham, United Kingdom*  
(Received 2 December 2002; published 23 April 2003)

We describe analytical and numerical methods for calculating forces between conductors due to variations of electrostatic surface potential across their surfaces. In the simple case where the spatial variation of surface potential gives rise to uniform power spectra, we show that the electrostatic force can be large in comparison with, and scale in approximately the same way with distance of closest approach as, the Casimir force. Patch potentials that are consistent with existing experimental data could give rise to forces with a magnitude of 4% of the Casimir force at separations of 0.1  $\mu\text{m}$ .

DOI: 10.1103/PhysRevLett.90.160403

PACS numbers: 41.20.Cv

*Introduction.*—The electrostatic potential at the surface of a metal relative to its interior depends on the magnitude of the surface dipole moment per unit area which, in turn, depends on the separation of the lattice planes that are parallel to the surface [1]. Variation of the crystallographic directions exposed at the surface of a clean polycrystalline metal results in a variation of surface potential. This is referred to as the “patch effect.” Patch potentials are also generated and influenced by surface contamination and, in the case of alloys, by variations in chemical composition. Differences in the mean potential of two connected metals are referred to as contact potential differences. Forces due to contact potentials are relatively easily calculated as they lead to long range electrostatic forces equivalent to those between the plates of a biased capacitor and will not be discussed further here.

There is considerable interest at present in performing ultrahigh sensitivity mechanical experiments [2–6]. All these experiments or applications are sensitive to the forces between metallic objects and are therefore susceptible to the electrostatic forces generated by patch-potential variations. Of particular importance are Casimir force experiments, as these measure directly the mechanical pressure resulting from the QED vacuum state. Here we will only study the implications of electrostatic background forces for Casimir force experiments where conductor separations are in the range of 0.1 to 1  $\mu\text{m}$ . The general methods developed here can be applied to all the experiments referenced above.

In an extensive recent review of experimental and theoretical developments in the Casimir force no mention was made of the possible influence of forces due to patch-potential variations [2]. The authors concluded that, at present, experimental determinations of the Casimir force have an accuracy of about 1% and speculated on future improvements of several orders of magnitude. In at least two separate measurements of the Casimir force it is explicitly assumed that, in the relevant geometry, patch-potential variations give rise to forces that vary as  $1/a^2$  where  $a$  is the minimum separation [7,8]. It is therefore

concluded that these forces can be distinguished from the Casimir force, which varies essentially as  $1/a^3$ . We show here that this conclusion is not necessarily correct.

*Observed variations of surface potentials.*—Patch potential variations are specific to the particular sample and dependent on environmental factors. Spatial variations of surface potentials are expected to be related to the physical size of the surface crystallites, which in the case of bulk metals, are typically of the order of 1  $\mu\text{m}$ . In the case of thin films, deposited on substrates at temperatures much less than the melting point of the film, the film is amorphous, has a nonuniform thickness and the crystallite size is of the same order as the thickness of the film [9]. Annealing of the film can produce grain structure that is substantially larger than its thickness. Patch-potential variations have been measured under various conditions using vibrating or rotating plate electrometers [10]. Notably it was shown that large-scale variations in surface potential were caused by adsorption of contaminants which was transient and found to *reduce* the variation of surface potential of the clean surfaces [8,11]. Unfortunately the concentration of contaminants may be unstable or unknown in any particular experiment.

Many experiments use thermally evaporated thin films of gold [12]. The work functions of gold are 5.47, 5.37, and 5.31 eV for the  $\langle 100 \rangle$ ,  $\langle 110 \rangle$ , and  $\langle 111 \rangle$  direction, respectively [13]. If the surfaces are clean and amorphous then we can assume that they comprise equal areas of these three crystallographic planes, and the variance,  $\sigma_v^2$ , of the potential distribution becomes approximately  $(90 \text{ mV})^2$ . When annealed, gold thin films form mesa structures with the  $\langle 111 \rangle$  crystallographic planes exposed. In this case, variations of surface potential are presumably generated by the material lying between the mesas. The size of the mesas depends on the temperature of the substrate during the formation of the film.

Sukenik *et al.*, observed rms variations of electric field due to thermally evaporated gold using the Stark effect in sodium atoms [14,15]. The films were partially optically transparent with a thickness of 42 nm and heated at 120 °C for several hours in vacuum. They deduced the

magnitude of the surface potentials to be 150 mV assuming the scale of variation to be of the order of the film thickness. This film thickness is significantly less than the plasma wavelength and so would not be suitable for determinations of the Casimir force. The plasma wavelength,  $\lambda_p$ , of gold is 136 nm.

*Calculation of patch forces.*—We suppose that we have two infinite parallel conducting surfaces normal to the  $z$  direction, separated by a distance  $a$ , with observable potential variations,  $v_i(\vec{x}_i)$ . The two-dimensional correlation functions can be defined as

$$c_{ij}(\vec{x}) = \iint v_i(\vec{\xi})v_j(\vec{\xi} - \vec{x})d^2\xi, \quad (1a)$$

with Fourier coefficients

$$C_{ii} = V_i(\vec{k})V_i(-\vec{k}). \quad (1b)$$

We define the symmetric components of the shifted cross-correlation function as

$$C_{12}(\vec{k}, \vec{\chi}) = \frac{1}{2}(V_1(-\vec{k})V_2(\vec{k})e^{i\vec{k}\cdot\vec{\chi}} + V_1(\vec{k})V_2(-\vec{k})e^{-i\vec{k}\cdot\vec{\chi}}), \quad (1c)$$

where  $\vec{\chi}$  is a displacement between the origins of the coordinate systems  $\vec{\chi} = \vec{x}_2 - \vec{x}_1$ .

In our model the patch potentials are generated by planes of dipoles of varying moment per unit area that lie adjacent to perfectly conducting equipotential surfaces (see Fig. 1). The substrates represent the electronic states within the metal that lie at the Fermi surface.

The membranes, of dipole moment  $m_1(\vec{x}_1)$  and  $m_2(\vec{x}_2)$ , are located at  $z_1 = \delta$  and  $z_2 = a - \delta$ , respectively, and the grounded planes are located at  $z = 0$  and  $a$ . The volume bounded by the conducting planes is a closed system with no extra sources of energy. We can calculate the electrostatic energy within the region  $0 < z < a$  as

$$\Phi_e = \frac{\epsilon_0}{2} \iiint \vec{E}^2 d^3\vec{x} dz. \quad (2)$$

$$\phi(\vec{x}, z) = \frac{1}{(2\pi)^2} \iint \frac{\cosh(k_z \delta)}{\sinh(k_z a)} \{M_1(\vec{k}) \sinh[k_z(a-z)]e^{i\vec{k}\cdot\vec{x}_1} - M_2(\vec{k}) \sinh(k_z z)e^{i\vec{k}\cdot\vec{x}_2}\} d^2\vec{k}. \quad (6)$$

Substituting into (5) we find

$$\Phi_e = -\frac{1}{2(2\pi)^2} \iint \frac{\cosh(k_z \delta)}{\sinh(k_z a)} \{(M_{11} + M_{22}) \cosh[k_z(a-\delta)] + 2M_{12} \cosh(k_z \delta)\} d^2\vec{k}, \quad (7)$$

where the Fourier coefficients of the correlation functions of the dipole moment distributions are given in an analogous way to Eqs. (1a)–(1c).

In the limit that  $\delta \rightarrow 0$ , Eq. (6) is the potential within the region of interest with boundary potentials  $v_1(\vec{x})$  and  $v_2(\vec{x})$ . We conclude that in this limit  $m_1(\vec{x}) = v_1(\vec{x})$  and  $m_2(\vec{x}) = -v_2(\vec{x})$ , explicitly confirming the expectation that variation in surface potential can be equated to a variation in the dipole moment per unit area and giving a

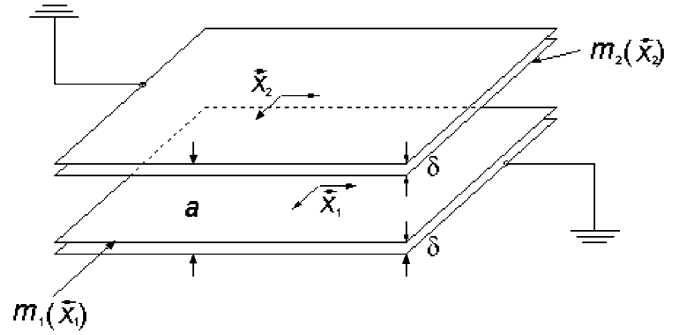


FIG. 1. Real metallic surfaces are modeled as membranes of varying dipole moments  $m_i(x_i)$ , adjacent to equipotential substrates.

We now use the identity

$$\nabla \cdot (\phi \vec{E}) = \vec{E} \cdot \nabla \phi + \phi \nabla \cdot \vec{E}. \quad (3)$$

The volume integral of the term on the left can be written as a surface integral at the boundary of integration and, recalling that this potential is zero, we can rewrite Eq. (2) as

$$\Phi_e = \frac{\epsilon_0}{2} \iiint \phi \nabla \cdot \vec{E} d^3\vec{x} dz. \quad (4a)$$

As the only sources of the electrostatic field within the volume of integration are the dipole layers,

$$\nabla \cdot \vec{E} = \frac{\sigma(\vec{x})}{\epsilon_0} [\delta(z - (z_i + \Delta)) - \delta(z - (z_i - \Delta))], \quad (4b)$$

where  $2\Delta$  is the small separation between the surface charges that comprise the dipole layer, we obtain

$$\Phi_e = \frac{1}{2} \sum_{i=1,2} \iint \vec{m}_i(\vec{x}_i) \cdot \nabla \phi(z_i) d^2\vec{x}_i, \quad (5)$$

where  $m_i(\vec{x}) \equiv 2\Delta\sigma_i(\vec{x})$ . We use the method of images to find the potential,  $\phi(\vec{x}, z)$ , in the region  $\delta \leq z \leq a - \delta$ . Each dipole layer produces an infinite set of images, the sum of the potentials due to these images converges to give

strong physical basis for the model. In this limit the electrostatic energy becomes

$$\Phi_e = -\frac{\epsilon_0}{2(2\pi)^2} \iint \frac{k_z}{\sinh(k_z a)} [(C_{11} + C_{22}) \cosh(k_z a) - 2C_{12}] d^2\vec{k}. \quad (8)$$

The force acting between the two infinite planes follows as  $F_p = -\partial\Phi_e/\partial a$ ;

$$F_p = -\frac{\epsilon_0}{2(2\pi)} \iint \frac{k_z^2}{\sinh^2 k_z a} [C_{11} + C_{22} - 2C_{12} \cosh(k_z a)] d^2 \vec{k}. \quad (9)$$

Provided that the separation of the plates is small compared to their horizontal extent, we would expect Eq. (9) to give a good estimate of the force acting between finite plates in terms of the spatial distributions of surface potentials. Transverse forces can also be calculated in a straightforward manner and are finite only when the two surface potentials are correlated [16].

The favored electrode geometry for the precision determination of the Casimir force is a sphere and a plane (although we note that a Casimir experiment with parallel plates has been reported in [17]). It is clearly difficult to apply the above method to such a geometry. However, provided that the energy of interaction,  $\Phi_n$ , between the planes, is invariant with respect to the lateral translation of the planes, we can employ the PFT [18]. We calculate the interaction energy by removing from Eq. (8) the potential energy at infinite separation, which is simply the self-energy of the two dipole distributions. We find

$$\Phi_n = -\frac{\epsilon_0}{2(2\pi)^2} \iint \frac{k_z [(C_{11} + C_{22})e^{-k_z a} - 2C_{12}]}{\sinh(k_z a)} d^2 \vec{k}. \quad (10)$$

It is now convenient to normalize the correlation and cross-correlation spectra [Eqs. (1a)–(1c)] by the area,  $S$ , over which the integrals are being evaluated. We then define  $\tilde{C}_{ij} = C_{ij}/S$ , where  $\tilde{C}_{ij}$  are measured in units of  $V^2/(\text{rad m}^{-1})^2$  and are essentially power spectral densities [4,7]. The PFT then gives the attractive force between a plane and a convex surface of radius  $R$  as

$$F_s = -\frac{\pi \epsilon_0 R}{(2\pi)^2} \iint \frac{k_z [(\tilde{C}_{11} + \tilde{C}_{22})e^{-k_z a} - 2\tilde{C}_{12}]}{\sinh(k_z a)} d^2 \vec{k}. \quad (11)$$

In the limit that  $k_z a \ll 1$  Eq. (9) gives the force between the plates of a biased parallel plate capacitor. In the same limit Eq. (11) gives the expected expression for the attractive force between a plane and a sphere for  $R \gg a$  [19].

In the limit that  $k_z a \ll 1$  forces are attractive irrespective of the relative polarity of the surface dipole distributions. However, in the limit that  $k_z a > 1$  and when opposite polarities of dipoles are adjacent, a repulsive force is produced.

In order to handle more general geometries, where the above methods cannot be applied, we have developed a discrete element method that enables us to deal with arbitrary surface potential distributions in arbitrary geometries. In analogy with the physical picture presented above, the surface of a real metallic object is modeled to be composed of a surface dipole layer and an ideal equipotential metal surface underneath. Given a particular surface potential distribution, electrostatic surface

charges are found on the metallic surfaces so that appropriate boundary conditions on the total electric field are fulfilled. The resulting forces are easily computed.

*Estimate of the force due to random variations in patch potentials.*—We will first derive some worst case limits on the magnitude of the patch force for uncontaminated surfaces. Using Parseval's theorem we can relate the correlation coefficients to the variance

$$\sigma_v^2 = \frac{1}{S} \iint V(\vec{x})^2 d^2 \vec{x} = \frac{1}{(2\pi)^2} \iint \tilde{C}_{ii}(k) d^2 \vec{k}. \quad (12)$$

In order to make progress we will assume a two-dimensional distribution of voltages whose Fourier coefficients lie within an annulus in two-dimensional  $k$  space ( $k_x, k_y$ ) with  $k_{\min} < |k| < k_{\max}$  and  $k_z = |k|$ . We will also assume that spatial distributions of potentials are uncorrelated which implies that  $\tilde{C}_{12}$  vanishes. The force per unit area between two parallel plates becomes

$$f_p = -\frac{2\epsilon_0 \sigma_v^2}{(k_{\max}^2 - k_{\min}^2)} \int_{k_{\min}}^{k_{\max}} \frac{k^3}{\sinh^2 ka} dk, \quad (13)$$

and the force between a sphere and a plane becomes

$$F_s = -\frac{4\pi \epsilon_0 \sigma_v^2 R}{(k_{\max}^2 - k_{\min}^2)} \int_{k_{\min}}^{k_{\max}} \frac{k^2 e^{-ka}}{\sinh ka} dk. \quad (14)$$

The integrands in Eqs. (13) and (14) have maximum values when  $ka \approx 1.3$  and  $ka \approx 0.8$ , respectively. In order to examine *the worst case* we will select the central wavelength of the spectrum that maximizes the forces due to the patch potentials for a nominal separation of  $1 \mu\text{m}$ . We will assume gold surfaces with  $\sigma_v^2 = (90 \text{ mV})^2$  and set the width to extend over a decade in spatial frequency. This is somewhat arbitrary but not unphysical. A plot of the resulting  $f_p$  is shown in Fig. 2(a). We also plot in Fig. 2(a) the Casimir force per unit area acting between two plane, parallel plates,  $f_{cp} = -\eta(a)(\pi^2 \hbar c / 240 a^4)$  where  $\eta(a)$  is an approximate empirical factor that reduces the magnitude of the Casimir effect due to the finite plasma frequency. We take  $\eta(a) = [1 + (8\lambda_p / 3\pi a)]^{-1}$  following [20].

At  $1 \mu\text{m}$  separation the patch force varies with separation in a way that roughly mimics the Casimir force and the ratio of the  $f_p/f_{cp}$  is approximately 11.

Figure 2(b) shows the Casimir and patch-potential forces as a function of closest separation,  $a$ , for the sphere/plane geometry and a worst case wavelength spectral range between 2.5 and  $25 \mu\text{m}$ . In this case the Casimir force is  $F_{cs} = \eta(a)(2\pi R/3)(\pi^2 \hbar c / 240 a^3)$ . In the figure we have assumed a radius of the spherical surface of 10 cm. The ratio of patch to Casimir force is independent of this choice. Again the patch-potential variation with separation mimics the Casimir force and the ratio of patch-field force to Casimir force,  $F_s/F_{cs}$ , is about 30 at  $a = 1 \mu\text{m}$ . In both Figs. 2(a) and 2(b) plots of the forces expected due to uniform voltage differences across the conductors are also shown.

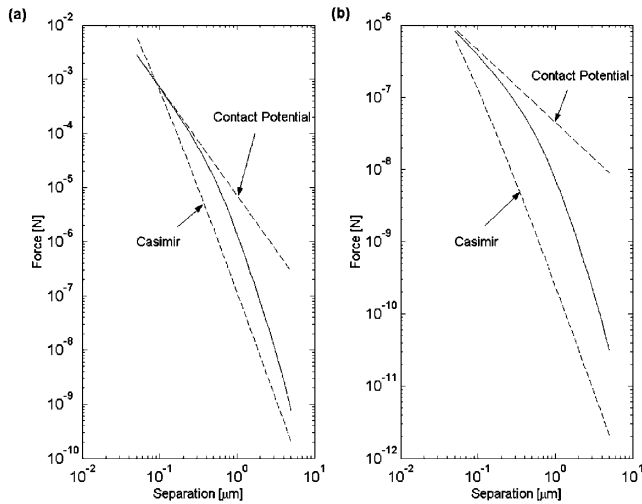


FIG. 2. (a) Force between parallel plates and (b) between a sphere and a plane for patch potentials with variance  $\sigma_v = 90$  mV and uniform power spectra. The Casimir force and the force due to a uniform potential difference  $\sigma_v$  are also shown.

The results of Sukenik *et al.* are consistent with a range of wavelengths between  $0.08$  and  $0.8 \mu\text{m}$  and  $\sigma_v \approx 76$  mV. The patch force then amounts to 4% of the Casimir force for a separation of  $0.1 \mu\text{m}$  and would scale with separation as  $1/a^{3.5}$ . If we assume that the wavelengths present in the spectrum scale with film thickness but that  $\sigma_v$  is invariant, we find the patch force is 50% of the Casimir force at  $0.1 \mu\text{m}$  separation and varies approximately as  $1/a^3$ , for films of  $140$  nm thickness.

*Forces due to large-scale variations in patch-potential.*—We can quantify the effect of surface contamination by regarding the process as a dynamic exchange of molecules between the surface and the space above. At a particular point  $p$  on the surface, the density of molecules can be considered to be proportional to the open solid angle available to them,  $\Omega(p)$  [11]. The attenuating effect of the contaminants can be modeled by covering the interacting surfaces with a dipole layer of density  $\rho(p) = \frac{A}{\epsilon_0} [1 - \Omega(p)/2\pi]$ . We have used the numerical method described above to study two specific geometries employed in previous Casimir force experiments. The first comprised a truncated spherical shell in front of a planar disc of lateral extent comparable to that of the shell [9]. The second consisted of a small sphere in front of a grounded plane of essentially infinite extent [11]. For a conservative choice of  $A$  of  $10$  mV, the force due to adsorbates amounts to 0.5% of the Casimir force at  $1$  mm for the first geometry, and 0.25% at  $0.1 \mu\text{m}$  for the second. The forces due to adsorbates scale approximately as  $1/a^{1.0}$  and  $1/a^{0.9}$ , respectively, for each geometry and should therefore be easily distinguishable from Casimir forces. They may, however, significantly modify the scaling at relatively large  $a$ , which is usually assumed to correspond to spatially constant potentials across the electrodes.

*Conclusions.*—We cannot claim that the results presented here accurately reflect any real experiment as the scaling of the patch force with gap depends crucially on the range of spatial wavelengths present in the spectrum. In the absence of such data, we have simply calculated the plausible magnitude of patch forces that are consistent with published results. However, our results suggest that patch forces should be considered as sources of systematic uncertainty in precise experimental determinations of the Casimir force. We have shown that forces due to larger scale potential variations due to contamination produce forces that scale differently to Casimir force and should therefore be less problematic.

Clearly it would be desirable to measure the relevant patch-potential variations *in situ*. We note that techniques based on Kelvin electrometers and probes appear to offer sufficient resolution and sensitivity for this application [21,22].

We are grateful to Quanmin Guo, Astrid Lambrecht, Serge Renaud, and Peter Bender for useful discussions. We thank BAE Systems and the Leverhulme Trust for financial support for this work.

- 
- [1] N. D. Lang and W. Kohn, Phys. Rev. B **3**, 1215 (1971).
  - [2] M. Bordag, U. Mohideen, and V. M. Mostepanenko, Phys. Rep. **353**, 1 (2001).
  - [3] LISA Pre-Phase A Report, 1998, available at <http://lisa.jpl.nasa.gov>
  - [4] P. W. Worden, C. W. F. Everitt, and M. Bye, STEP Science Requirement Document, Stanford, 1990.
  - [5] C. D. Hoyle, *et al.*, Phys. Rev. Lett. **86**, 1418 (2001).
  - [6] H. B. Chan, Science **291**, 1941 (2001).
  - [7] S. K. Lamoreaux, Phys. Rev. Lett. **78**, 5 (1997).
  - [8] T. E. Ederth, Phys. Rev. A **62**, 062104 (2000).
  - [9] Z. H. Liu, N. M. D. Brown, and A. McKinley, J. Phys. Condens. Matter **9**, 59 (1997).
  - [10] F. Rossi and G. I. Opat, J. Phys. D **25**, 1349 (1992).
  - [11] U. Mohideen and A. Roy, Phys. Rev. Lett. **61**, 4549 (1998).
  - [12] B. W. Harris, F. Chen, and U. Mohideen, Phys. Rev. A **62**, 052109 (2000).
  - [13] *CRC Handbook of Chemistry and Physics*, edited by C. R. Lide (CRC Press, Boca Raton, FL, 2001), 82nd ed.
  - [14] C. I. Sukenik, *et al.*, Phys. Rev. Lett. **70**, 560 (1993).
  - [15] V. Sandogdhar, *et al.*, Phys. Rev. Lett. **68**, 3432 (1992).
  - [16] C. C. Speake, Classical Quantum Gravity **13**, A291 (1996).
  - [17] G. Bressi *et al.*, Phys. Rev. Lett. **88**, 041804 (2002).
  - [18] B. Derjaguin, Kolloid Z. **69**, 155 (1934).
  - [19] W. R. Smythe, *Static and Dynamic Electricity* (Taylor and Francis, Bristol, United Kingdom, 1989), 3rd ed.
  - [20] A. Lambrecht and S. Reynaud, Eur. Phys. J. D **8**, 309 (2000).
  - [21] H. N. McMurray and G. Williams, J. Appl. Phys. **91**, 1673 (2002).
  - [22] J. B. Camp, T. W. Darling, and R. E. Brown, J. Appl. Phys. **69**, 7126 (1991).